VERSITA

OPTO-ELECTRONICS REVIEW **15**(4), 223–228

DOI: 10.2478/s11772-007-0024-6

Wavelength and polarization selective multi-band tunnelling quantum dot detectors

A.G.U. PERERA*[1], G. ARIYAWANSA[1], V.M. APALKOV[1], S.G. MATSIK[1], X.H. SU[2], S. CHAKRABARTI[2], and P. BHATTACHARYA[2]

[1]Department of Physics and Astronomy, Georgia State University, Atlanta, GA 30303, USA
[2]Department of Electrical Engineering and Computer Science, University of Michigan, Ann Arbor, Michigan 48109-2122, USA

The reduction of the dark current without reducing the photocurrent is a considerable challenge in developing far-infrared (FIR)/terahertz detectors. Since quantum dot (QD) based detectors inherently show low dark current, a QD-based structure is an appropriate choice for terahertz detectors. The work reported here discusses multi-band tunnelling quantum dot infrared photo detector (T-QDIP) structures designed for high temperature operation covering the range from mid- to far-infrared. These structures grown by molecular beam epitaxy consist of a QD (InGaAs or InAlAs) placed in a well (GaAs/AlGaAs) with a double-barrier system (AlGaAs/InGaAs/AlGaAs) adjacent to it. The photocurrent, which can be selectively collected by resonant tunnelling, is generated by a transition of carriers from the ground state in the QD to a state in the well coupled with a state in the double-barrier system. The double-barrier system blocks the majority of carriers contributing to the dark current. Several important properties of T-QDIP detectors such as the multi-colour (multi-band) nature of the photoresponse, the selectivity of the operating wavelength by the applied bias, and the polarization sensitivity of the response peaks, are also discussed.

Keywords: multi band, IR detectors, quantum dot, resonant tunnelling, polarization.

1. Introduction

With the increasing interest in the terahertz region of the spectrum (0.1–3.0 THz) for applications in imaging, communication, security and defence, there is a need for terahertz detectors exhibiting low dark current and high operating temperatures. One of the challenges in developing terahertz detectors is the reduction of the dark current (due to thermal excitations) associated with terahertz detection mechanisms. At the present time, terahertz detectors such as Ge BIB detectors [1], photo conductors triggered by femtosecond laser pulses [2], quantum well detectors [3], hetero junction detectors [4], and thermal detectors, such as bolometers and pyroelectrics all of which operate at low temperatures, are being studied. A typical detector structure, in which the transitions leading to terahertz detection occur between two electronic states with an energy difference of ΔE (4.1 meV for 1 THz), would not be suitable for high temperature terahertz detection since the thermal excitations become dominant even at 77 K due to small ΔE. Quantum dot (QD) based detectors inherently show low dark currents, offering a suitable platform for high operating temperature terahertz detectors. In order to decrease the dark current further, a tunnelling quantum dot infrared photo detector (T-QDIP) structure was studied [5]. Successful results on a two-colour T-QDIP with photoresponse peaks at 6 μm and 17 μm operating at room temperature [5], and a terahertz T-QDIP responding [6] at 6 THz (50 μm) for a temperature of 150 K have been previously reported. In the T-QDIP structure grown by molecular beam epitaxy (MBE), a QD (InGaAs or InAlAs) is placed in a well (GaAs/AlGaAs) with a double-barrier system (AlGaAs/InGaAs/AlGaAs) adjacent to it. The photocurrent generated by a transition from the ground state in the QD to a state in the well (denoted as resonant state as this state is considered for resonance tunnelling) coupled with a state in the double-barrier system can be collected by resonant tunnelling, while the double-barrier system blocks the majority of the carriers contributing to the dark current (carriers excited to any state other than the resonant state in the well). Two important properties of the T-QDIP detectors are the selectivity of the operating wavelength and the multi-colour (band) nature of the photoresponse based on different transitions in the structure. Furthermore, the wavelength bands in a dual-band T-QDIP resulting from transitions between the QD ground state and two QD excited states coupled with states in the double-barrier system (i.e., two resonant states) can be tuned by varying the bias voltage due to the dependence of resonance conditions for each resonant state on the applied bias. This allows for sep-

*e-mail: uperera@gsu.edu

aration of the photo current generated by two response bands, without using external filters. The multi-band nature of T-QDIPs would be useful for applications such as mine detection [7], where scanning in two different wavelength bands greatly enhances detection capabilities and reduces false positives.

2. Tunnelling quantum dot structures: background

The low quantum efficiency associated with reduced photo current is a major constraint with conventional terahertz detector structures designed to use above cryogenic temperatures. This is due to the fact that structures normally designed to reduce the dark current could reduce the photo current as well. A T-QDIP structure, which uses resonant tunnelling to selectively collect the photo current generated within the quantum dots, while the tunnelling barriers block the majority of thermally excited carriers contributing to the dark current, would be an appropriate choice for the development of high performance high operating temperature detectors. The schematic diagram of a T-QDIP structure (labelled as MG386) is shown in Fig. 1(a), and the conduction band profiles under zero bias and under an applied reverse bias are shown in Fig. 2(a) and (b), respectively. The structure was grown by molecular beam epitaxy (MBE), with the GaAs and AlGaAs layers grown at 610°C and the InGaAs QD layers grown at 500°C on a GaAs layer. $Al_{0.3}Ga_{0.7}As/In_{0.1}Ga_{0.9}As/Al_{0.3}Ga_{0.7}As$ serves as the double-barrier system. Vertical circular mesas for top illumination were fabricated by standard photolithography, wet chemical etching and contact metallization techniques. The n-type top ring contact and the bottom contact were formed by evaporated Ni/Ge/Au/Ti/Au with thickness of 250/325/650/200/2000 Å. Radius of the optically active area is 300 μm. The structure was designed to include a bound state in the well, which can couple to another state in the double-barrier system. For carriers excited by radiation with energy equal to the energy difference between the QD ground state and the resonant state, the tunnelling probability can be shown to be near unity. Carriers excited into other states (contributing to the dark current) are blocked by the double-barrier system. In this way, a higher barrier for thermal excitations can be introduced, even though the photo excitation energy is very low. As a result, the operating temperature of the detector can be significantly increased. The operating wavelength can be tuned by changing the parameters that are associated with the QD and the well in the structure.

The QD energy levels are calculated by using 8-band **k.p** model [8]. This model takes into account the strain in the quantum dot calculated from the valence force field [9,10] (VFF) model, which has proven to be successful in calculating the strain tensor in self-assembled quantum dots. QD size and confinement potential should be determined in order to obtain required energy spacing between states in the QD. Energy states in the well, including the presence of the wetting layer and the double-barrier system, are calculated by solving the one-dimensional Schrödinger equation. The transmission probability for the double-barrier system is calculated using the transfer matrix method [11]. The width of the well and parameters of the double-barrier system are determined so the transitions from E_0, E_1, and E_2 states give rise to the expected peak wavelengths.

A comparison of the dark current density between quantum dots-in-a-well (DWELL) [12] and T-QDIP (MG386) detectors at 80 K is shown in Fig. 3. The dark current densities at a bias of –2 V are 3×10^{-1} and 1.8×10^{-5} A/cm^2 for DWELL and T-QDIP, respectively. The reduction of the dark current of T-QDIP is associated with dark current blocking by the double-barrier system in the structure. The response of MG386 showing two-colour response at wavelengths of ~6 and ~17 μm up to room temperature was recently reported [5]. The spectral response measured at 80 K under different bias values are shown in Fig. 4, and the responsivity at 300 K under –2 V bias is shown in the inset. The peak responsivity and the quantum efficiency of

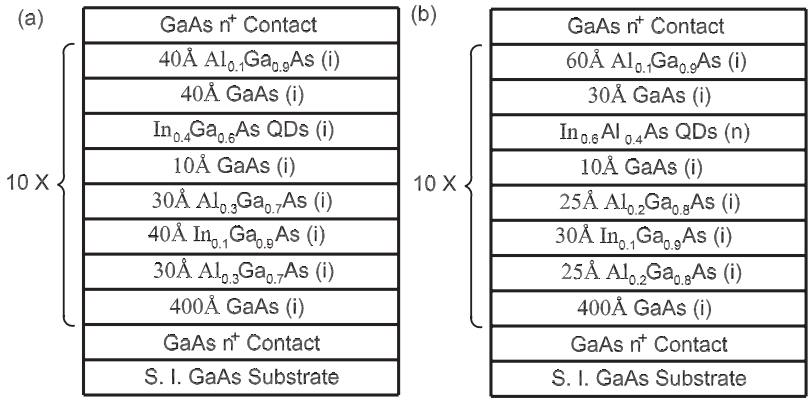

Fig. 1. Layer architecture of two different T-QDIP structures, (a) MG386 and (b) MG764, grown by MBE. QDs (InGaAs or InAlAs) are formed by self-assembled process. $Al_{0.3}Ga_{0.7}As/In_{0.1}Ga_{0.9}As/Al_{0.3}Ga_{0.7}As$ and $Al_{0.2}Ga_{0.8}As/In_{0.1}Ga_{0.9}As/Al_{0.2}Ga_{0.8}As$ serve as double-barrier systems for MG386 and MG764, respectively. In MG764 structure, InAlAs was used instead of InGaAs to grow smaller QDs, and the average size of QDs was found to be 140/40 Å (base dimension/height).

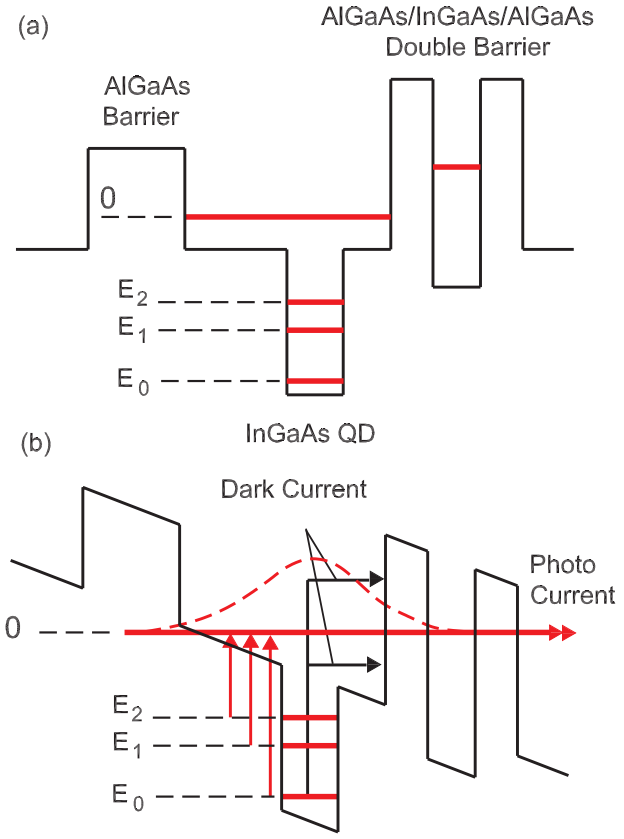

Fig. 2. Schematic diagram of the conduction band profile of MG386 T-QDIP structure under (a) zero bias and (b) reverse bias. The energy level positions in the QD with respect to the resonant state are denoted by E_0, E_1, and E_2. Only the carriers excited to the resonant state will contribute to the current. Hence, most of the dark current will be blocked, except the thermal excitations on to the resonant state. The resonance condition is possible only under an applied bias when there is an overlap between the resonant state and the state in the double-barrier system.

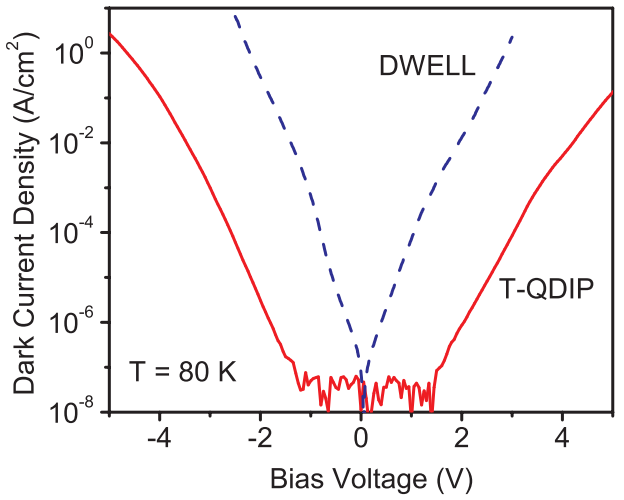

Fig. 3. A comparison of the experimental dark current density between DWELL [12] and T-QDIP detector (MG386) at 80 K. The reduction of the dark current in T-QDIP is attributed to dark current blocking by tunnelling barriers.

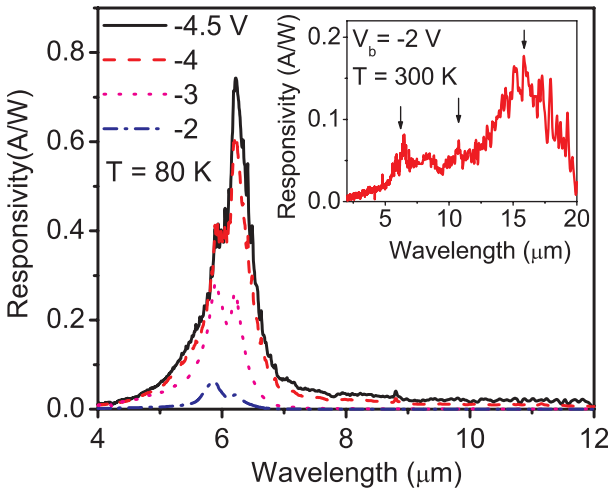

Fig. 4. Response of the MG386 T-QDIP detector at 80 K under different bias voltages. The response at 300 K is shown in the inset. The arrows represent the positions of the peaks resulted from different transitions in the structure. The peaks at 11 and 17 μm are possible only at high temperatures since the transitions leading to these peaks are enabled by the carrier occupancy in the states E_1 and E_2, which occur at high temperatures.

the 6-μm peak at 80 K and –4.5 V are ~0.75 A/W, and 16%, respectively. The calculated energy level positions E_0, E_1, and E_2 are equal to –161, –102, and –73 meV. Hence, it can be confirmed that the peak at ~6 μm is due to transitions from the ground state of the dot E_0 to the resonant state in the well (ΔE = 161 meV). At 300 K, the 17-μm peak results from transitions from the state E_2 to the resonant state (ΔE = 73 meV). Due to the symmetry of the dot geometry, the excited states in the QDs have a higher degeneracy (8) than the ground state (2). Therefore, the number of carriers in the excited states, compared to that in the ground state, increases with temperature. As a result, the 17-μm peak is dominant at high temperatures. The weak response at ~11 μm corresponds to the energy separation between the E_1 state and the resonant state (ΔE = 102 meV). Furthermore, the specific detectivity, D^*, at 17 μm is on the order of 10^7 cmHz$^{1/2}$/W at 300 K, while D^* for the 6-μm peak is 2.4×10^{10} cmHz$^{1/2}$/W for a bias of 2 V at 80 K.

3. Tunnelling quantum dot terahertz detectors

Using the resonant tunnelling approach, successful results were reported [6] on a terahertz T-QDIP detector (MG764) responding at 6 THz (50 μm) for a temperature of 150 K. In order to obtain a transition leading to a response in the terahertz region, smaller n-doped QDs having two-bound states were used in the structures. As a result, the energy separation between the second state in the quantum dot and the resonant state in the well was reduced, while doping raised the Fermi level above the second state in the QD. Layer architecture of the structure is shown in Fig. 1(b). In this structure, InAlAs was used instead of InGaAs in order to grow smaller QDs with the average size of QDs found to

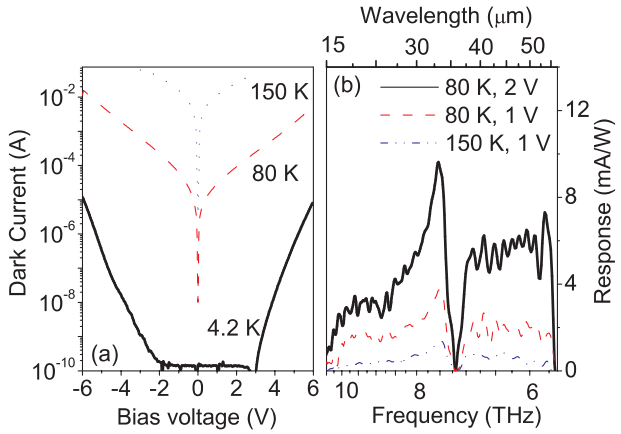

Fig. 5. Dark current (a) and spectral response (b) of MG764 terahertz T-QDIP detector at different temperatures. The peak at 6 THz is due to transitions of carriers from the QD ground state to the resonant state. High temperature response was made possible by resonant tunnelling. The broadening of the peak, FWHM ~23 meV (30 μm), is attributed to inhomogeneous broadening (up to 40 meV) due to size fluctuation of QDs.

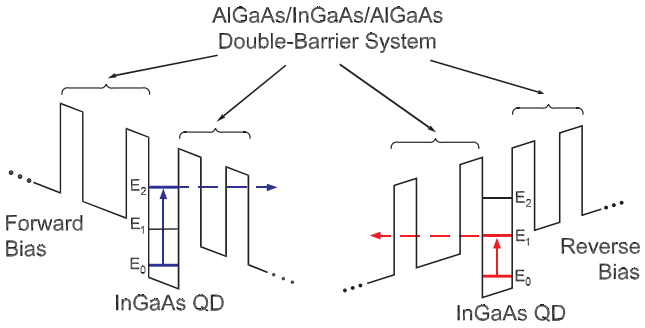

Fig. 6. Band diagram of the dual-band T-QDIP detector under 1.5 kV/cm forward bias field and under 1.8 kV/cm reverse bias field. The structure consists of 13-nm diameter and 6-nm height $In_{0.6}Ga_{0.4}As$ QDs on a 2-nm thick wetting layer sandwiched between two double-barrier systems. The thickness of the well of the 10-nm $Al_{0.3}Ga_{0.7}As/In_{0.1}Ga_{0.9}As$/5 nm $Al_{0.3}Ga_{0.7}As$ double-barrier system is 3 nm on the forward side and 5 nm on the reverse side.

be 140/40 Å (base dimension/height). Experimental dark current and spectral response of the detector from 80 K to 150 K is shown in Fig. 5. The calculated energy difference between the two energy levels leading to the response is 24.6 meV (50.4 μm). The observed responsivity at 50.4 μm at 80 and 150 K are 6 and 0.6 mA/W, respectively. The full-width at half maximum (FWHM) of the spectral response is 23 meV (30 μm); this broadening arises due to the inhomogeneous size distribution of self-organized dots. Based on the obtained results, it can be concluded that the THz operation at high temperature (150 K) is made possible through the incorporation of resonant tunnelling phenomena into device design.

4. Dual-band wavelength selective T-QDIPs

The dual-band detection capability of a T-QDIP would be effective and efficient, if the two response bands could be selected without using external filters. In this article, a concept is proposed for a wavelength selective dual-band T-QDIP detector. Using two double-barrier systems on both sides of the QD, makes it possible to satisfy the resonant conditions for two excited states in the QD independently by applying either a forward or reverse bias. As the first step, the QD is designed to include two excited states, which provide the required energy spacing with respect to the ground state. For $In_{0.6}Ga_{0.4}As$ dots in $Al_{0.3}Ga_{0.7}As$ with 13-nm diameter and 6-nm height, the ground and first excited states in the x and z -directions are 154 (E_0), 241 (E_1), and 410 meV (E_2) above the conduction band of the dot. Even though there are additional excited states in the dot, they do not contribute to the photocurrent. The double-barriers are designed in order for the confined state in one double-barrier system to coincide with E_1, while that of the other double-barrier system coincides with E_2. The band diagram and expected response of a possible dual-band T-QDIP structure are shown in Figs. 6 and 7 under forward and reverse biases. The double-barrier system consists of a 10-nm thick $Al_{0.3}Ga_{0.7}As$ layer adjacent to the QD, a 3- or 5-nm $In_{0.1}Ga_{0.9}As$ layer, and a 5-nm thick $Al_{0.3}Ga_{0.7}As$ layer, providing a quantum well having a well width determined by the thickness of the $In_{0.1}Ga_{0.9}As$ layer. In this structure, the state in the 3-nm well double-barrier system coincides with the E_2 state under forward bias providing resonant conditions to the transitions from the E_0 to the E_2 state resulting in 4.8-μm response. Similarly, under reverse bias the confined state in the 5-nm well double-barrier system coincides with the E_1 state, providing resonant conditions to the transition leading to 14.3-μm re-

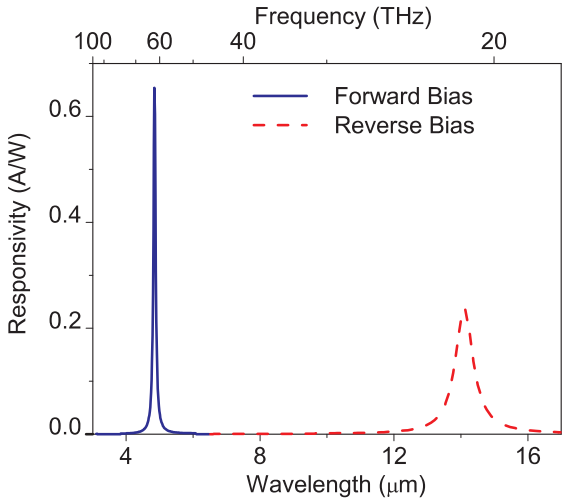

Fig. 7. Response of the proposed dual-band T-QDIP detector under 1.5 kV/cm forward bias field (4.8 μm) and under 1.8 kV/cm reverse bias field (14.3 μm). As shown, by changing the bias direction, the desired wavelength peak can be selected. Since the transmission of the higher energy state is better than that of the lower energy state due to the higher effective barrier for the lower state, the responsivity of the 14.3 μm peak is lower.

sponse. Since, only one response peak is possible at a time, peaks can be selected by changing the polarity of the applied bias. Since the transmission of the higher energy state is better than that of the lower energy state due to the higher effective barrier for the lower state, the responsivity of the 14.3-μm peak is lower than 4.8-μm peak. Increasing the number of QD layers as well as QD density enhance the absorption in the active region leading to higher responsivity. Introducing a gain mechanism into the structure will also increase the responsivity and enables high temperature operation. Evidence of high gain related to the phonon bottleneck and other transport/capture properties have been reported in the literature [13].

5. Dual-band polarization sensitive T-QDIPs

At present, polarization-sensitive detection technology has been a subject for infrared imaging, where the contrast between the target and its background is low. Polarization-sensitive infrared cameras have been investigated as a new technology for land mine detection [14,15]. QD-based structures can also be used to develop polarization sensitive detectors [16]. Here, a modification of T-QDIP structures is proposed for polarization sensitive infrared detectors. In order to achieve this with normal incidence configuration, a metal grid is coupled to the front surface of the structure as shown in Fig. 8. A single element with a grid pattern is considered as a pixel. Since the QD distinguishes between in and out of plane polarization, but not the orientation of in-plane polarization, the light must be coupled to the QDs in a polarization sensitive manner in order to identify in-plane polarization. Similar to wire grid polarizers, the grid serves as a polarizer for the incident radiation leading to the ability to detect polarization for both the QD transitions being considered in the T-QDIP structure. As discussed in the Sec. 4, the transitions in the QDs have different preferred orientations for the electric field. The polarization effects from grid couple the *x*- and *y* -polarized radiation to transitions excited by normal incidence light, i.e., the transitions leading to 4.8 μm and 14.3 μm peaks. Here, *x*- and *y*-polarization refer to the polarization of incident light in *x* and *y*-directions, and the growth direction is considered as *z*-direction.

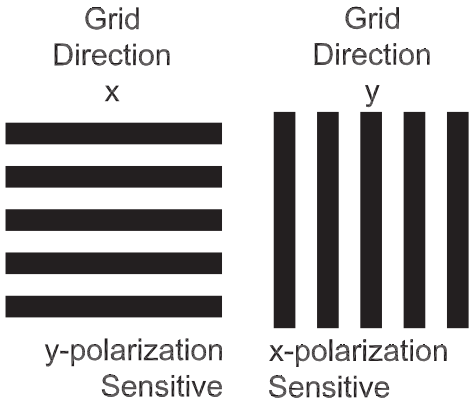

Fig. 8. The grid pattern on the surface of the T-QDIP detector to achieve polarization sensitivity. The grid directions correspond to the direction of the grid wires. The grid responds to light polarized perpendicular to the grid and grid direction *x* is sensitive to *y* -polarized light, while grid direction *y* is sensitive to *x*-polarized light.

The wavelength and polarization can be selected independently using the bias direction and the orientation of the grid on a given pixel. The responses shown in Fig. 7 are for polarization perpendicular to the grid. For polarization parallel to the grid, the response for both peaks would be zero. The combinations of grid and bias directions to select different wavelengths and polarizations are given in Table 1. By using adjacent pixels with the grids oriented perpendicularly, the polarization components could be selected. Switching the bias direction on the pixels allows the wavelength selection. Hence, the reported T-QDIP structure can be used as a wavelength selective polarization sensitive dual-band detector, which would open up a wide variety of applications.

Table 1. The combinations of grid and bias directions to select the different polarizations at the two wavelengths. The grid directions correspond to the direction of the grid wires, while the polariztion directions indicate the directions of the horizontal polarization of the incident radiation.

Grid Dir.	Bias Dir.	4.8 μm		14.2 μm	
		Polarization			
		x	*y*	*x*	*y*
x	Forward		√		
x	Reverse				√
y	Forward	√			
y	Reverse			√	

6. Conclusions

The development of multi-band and terahertz detectors using T-QDIP structures was discussed. The feasibility of wavelength selective dual-band TQDIPs was theoretically demonstrated. Furthermore, coupling a metal grid with the device structure can be used as a polarization sensitive detector, allowing wavelength-selective polarization-sensitive detection.

Acknowledgements

This work is supported in part by U.S. National Science Foundation (NSF) under the grant ECCS: 0620688.

References

1. E.E. Haller, "Advanced far-infrared detectors", *Infrared Phys*. **35**, 127–146 (1994).
2. M. Suzuki and M. Tonouchi, "Fe-implanted InGaAs photoconductive terahertz detectors triggered by 1.56 μm femtosecond optical pulses", *Appl. Phys. Lett*. **86**, 163504-3 (2005).

3. H.C. Liu, C.Y. Song, A.J. Spring Thorpe, and J.C. Cao, "Terahertz quantum-well photo detector", *Appl. Phys. Lett.* **84**, 4068 (2004).
4. M.B.M. Rinzan, A.G.U. Perera, S.G. Matsik, H.C. Liu, Z.R. Wasilewski, and M. Buchanan, "AlGaAs emitter/GaAs barrier terahertz detector with a 2.3 THz threshold", *Appl. Phys. Lett.* **86**, 071112 (2005).
5. P. Bhattacharya, X.H. Su, S. Chakrabarti, G. Ariyawansa, and A.G.U. Perera, "Characteristics of a tunnelling quantum-dot infrared photo detector operating at room temperature", *Appl. Phys. Lett.* **86**, 191106 (2005).
6. X.H. Su, J. Yang, P. Bhattacharya, G. Ariyawansa, and A.G.U. Perera, "Terahertz detection with tunnelling quantum dot intersublevel photodetector", *Appl. Phys. Lett.* **89**, 031117 (2006).
7. A. Goldberg, P.N. Uppal, and M. Winn, "Detection of buried land mines using a dual-band LWIR/LWIR QWIP focal plane array", *Infrared Physics & Technology* **44**, 427 (2003).
8. H. Jiang and J. Singh, "Strain distribution and electronic spectra of InAs/GaAs self-assembled dots: An eight-band study", *Phys. Rev.* **B56**, 4696 (1998).
9. R.M. Martin, "Elastic properties of ZnS structure semiconductors", *Phys. Rev.* **B1**, 4005 (1969).
10. P.N. Keating, "Effect of invariance requirements on the elastic strain energy of crystals with application to the diamond structure", *Phys. Rev.* **145**, 637 (1966).
11. E. Anemogiannis, N. Glytsis, and T.K. Gaylord, "Quasi-bound states determination using a perturbed wavenumbers method in a large quantum box", *IEEE. J. Quant. Electron.* **33**, 742 (1997).
12. S. Krishna, G. von Winckel, S. Raghavan, A. Stintz, G. Ariyawansa, S.G. Matsik, and A.G.U. Perera, "Three-colour (λ_{p1} ~3.8 μm, λ_{p2} ~8.5 μm, and λ_{p3} ~23.2 μm) InAs/InGaAs quantum dots in a well detectors", *Appl. Phys. Lett.* **83**, 2745 (2003).
13. J. Urayama, T.B. Norris, J. Singh, and P. Bhattacharya, "Observation of phonon bottleneck in quantum dot electronic relaxation", *Phys. Rev. Lett.* **86**, 4930 (2001).
14. M. Larive, L. Collot, S. Breugnot, H. Botma, and P. Roos, "Laid and flush-buried mines detection using 8–12 μm polarimetric imager", *Proc. SPIE* **3392**, 115 (1998).
15. B.A. Barbour, M.W. Jones, H.B. Barnes, and C.P. Lewis, "Passive IR polarization sensors: a new technology for mine detection", *Proc. SPIE* **3392**, 96 (1998).
16. B. Aslan, H.C. Liu, J.A. Gupta, Z.R. Wasiewski, G.C. Aers, S. Raymond, and M. Buchanan, "Observation of resonant tunnelling through a self-assembled InAs quantum dot layer", *Appl. Phys. Lett.* **88**, 043103 (2006).

